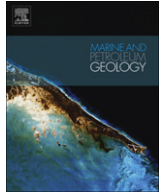


Contents lists available at [SciVerse ScienceDirect](http://www.sciencedirect.com)

# Marine and Petroleum Geology

journal homepage: [www.elsevier.com/locate/marpetgeo](http://www.elsevier.com/locate/marpetgeo)

## Geological model of the central Periadriatic basin (Apennines, Italy)

S. Bigi<sup>a</sup>, A. Conti<sup>a,\*</sup>, P. Casero<sup>b</sup>, L. Ruggiero<sup>a</sup>, R. Recanati<sup>c</sup>, L. Lipparini<sup>c</sup><sup>a</sup> Department of Earth Science, Sapienza University of Rome, P.le A. Moro 5, 00185 Rome, Italy<sup>b</sup> Via S. Martino Valperga 20, Roma, Italy<sup>c</sup> Medoilgas Italia S.p.A Via Cornelia n. 498, 00166 Rome, Italy

### ARTICLE INFO

#### Article history:

Received 8 February 2012

Received in revised form

23 July 2012

Accepted 27 July 2012

Available online xxx

#### Keywords:

3D modeling

Structural geology

Seismic lines

Seismic stratigraphy

Fold-and-thrust belt

Anticlines

Thrust basin

### ABSTRACT

3D geological models from multi-source data (cross-sections, geological maps, borehole logs and outcrops) are a critical tool to improve the interpretation of the spatial organization of subsurface structures that are not directly accessible. In this paper, we reconstruct the main geological structures and surfaces in three dimensions through the interpolation of closely and regularly spaced 2D seismic sections, constrained by wells data and surface geology. The methodology was applied in the Marche–Abruzzi sector of the Periadriatic basin, where the more external part of the Apennines fold-and-thrust belt is mostly buried under a syn- and post-orogenic, Plio–Pleistocene, siliciclastic sequence. The 3D model allowed us to correlate the main thrust fronts and related anticlines along strike, revealing a general ramp – flat – ramp trajectory characterizing the main structural trends. This geometric organization influences the sequence of thrust-system propagation and characterizes the evolution of syntectonic basins. The obtained 3D model points out several variation occurring along strike: i) main trends geometric relationships; ii) deformation chronology and iii) displacement distribution. In the northern sector, higher displacement and structural elevation are reached out by the Nereto–Bellante structure, whereas in the southern sector the Villadegna–Costiera Structure is the prevalent. All structures show a diachronic thrusts activity along strike, younger toward the north.

© 2012 Elsevier Ltd. All rights reserved.

### 1. Introduction

The development of software for 3D modeling (gOcad, Earth Vision, Move, Petrel among many others) has opened a new frontier in the Earth Sciences, leading to a more accurate spatial analysis of geological structure and to 3D models. Numerous papers deal with the integration of different kind of data for a 3D reconstruction of subsurface structures at a regional scale (Ledru, 2001 and references therein; Courrioux et al., 2001; Galera et al., 2003; Wu et al., 2005; Zanchi et al., 2009; Salvi et al., 2010). The subsurface data generally used for 3D reconstruction are the seismic data, integrated with well data log, techniques that has its maximum development in the hydrocarbon research (Fonnesu, 2000; Zampetti et al., 2004; Gee et al., 2007; among many others). Integrating geophysical and geological data, from seismic available database and by geological maps, is possible to define geometrical and geological constraints in order to create 3D surfaces, closed volumes and grids from the constructed objects.

In this work, we integrated 2D reflection seismic dataset, geological maps and borehole data to reconstruct the buried structures; this procedure provided the generation of 3D surfaces taking into account any geometrical constraint derived from the dataset.

The workflow followed three main steps. The first one was the construction of a digital database in a GIS environment, followed by the 2D interpretation of each seismic line; finally we built the main 3D stratigraphic and tectonic surfaces, working in a 3D space where the depth is expressed in TWT time. The depth conversion and restoration has been performed in 2D, along the most representative section derived from the 3D model. Most of the work was carried out with Kingdom 8.4 (Seismic Micro-Technology) for the seismic interpretation and Move 2011 (Midland Valley) for the reconstruction of the 3D model. We applied this approach to a wide sector of the Periadriatic Basin, between Ascoli Piceno to the north and Pescara to the south, at the front of the Apennines thrust belt system (Fig. 1). In this area, which has an extension of about 8000 km<sup>2</sup>, an extensive oil exploration activity has been carried out since '70–'80, and, as a consequence, the related seismic dataset is wide and mostly available, although not always of high quality (Videpi Project, 2009) (Fig. 2).

The structural setting of this area is the combination of extremely superficial thrust-related anticlines and their respective

\* Corresponding author.

E-mail addresses: [alessia.conti@uniroma1.it](mailto:alessia.conti@uniroma1.it) (A. Conti), [caseropiero@libero.it](mailto:caseropiero@libero.it) (P. Casero).

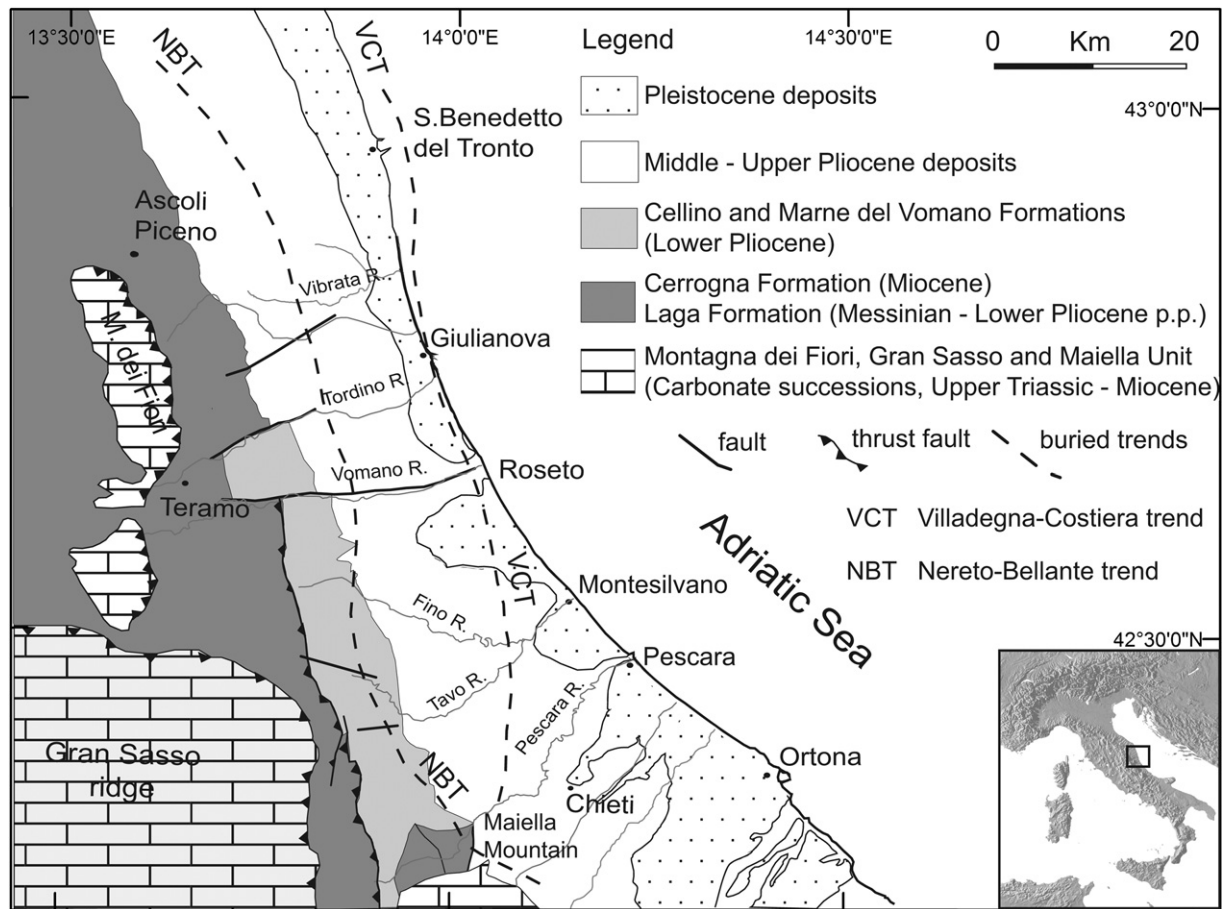


**Figure 1.** Geological map of the Central Periadriatic basin. The buried trends are the ones generally mapped in this area (from Structural Model of Italy, 1:1,000,000, modified).

deeper ramps, buried under syn- and post-orogenic, Plio-Pleistocene, siliciclastic sequences (Artoni and Casero, 1997; Argnani and Frugoni, 1997; Bigi et al., 2004; Carruba et al., 2006; Tozer et al., 2006).

A general evolution of the Periadriatic basin has been proposed, among many others, by Ori et al. (1991), Crescenti et al. (2004), Artoni (2007). Following Ori et al. (1991), the complex evolution of the Adriatic foredeep can be resumed in four stages: during the Messinian stage, the first one, the area was a typical foredeep basin (*sensu* DeCelles and Giles, 1996) where a single basin lie parallel to the structural axes of the mountain chain; the same basin was affected during the Early Pliocene by thrusting and a more internal and uplifted zone, still connected to the main basin, called “open piggy back basins” was defined. The third stage, in the Middle–Upper Pliocene, was characterized by an increase of tectonic activity; the fold-related fault grew up until they formed closed piggy back basins. In the last stage, no longer turbiditic deposition occurred and the area became a shallow water to continental depositional plane.

Although the described evolution has been recognized as a general trend by most of the Authors, a synthesis of the relationships among each single thrust related-fold throughout the basin is still a matter of debate. Most of the papers infact analyzed just a single sector of the basin whereas few or no works deal with the correlation of each thrust fronts along strike. There are infact unsolved aspect in terms of geometry, displacements and deformation chronology that can be highlighted by taking into account a bigger area of investigation and by the 3D reconstruction. Our 3D model showed that the two main N–S buried tectonic trends

(named Nereto–Bellante Trend and Villadegna–Costiera Trend) are characterized by deeper ramps in the carbonate sequence, long flats developed at their top, and shallower ramps and related anticlines involving the Plio–Pleistocene siliciclastic sequences. These trends are not cylindrical along strike and show different displacement distribution and chronology of deformation from north to south. The Nereto–Bellante Trend reaches the maximum offset and structural elevation in the northern sector, whereas the Villadegna–Costiera Trend progressively becomes the main structure moving to south; in addition, this latter has a very small displacement to the North, in contrast with the former that shows maximum displacement in the same sector. The thrusts activity results diachronic along strike and younger toward the north.

The reconstructed 3D model allowed to better define several features (displacement, chronology, plunging of the main trends) of the structural setting of the Periadriatic basin, hard to detect and visualize only with 2D seismic dataset. Moreover, the 3D approach improves our understanding of geological structures from the integration of multi-source data.

## 2. Geological setting

The Apennines are an E–NE verging fold-and-thrust belt developed since Late Oligocene and connected to the westward subduction of the continental Adria plate underneath the European plate (Malinverno and Ryan, 1986; Ricci Lucchi, 1986; Doglioni, 1991). Thrusts and related folds affected the Mesozoic–Tertiary carbonate sequence of the Adria continental margin; the over thrusting and uplifting of the Apennines was accompanied by

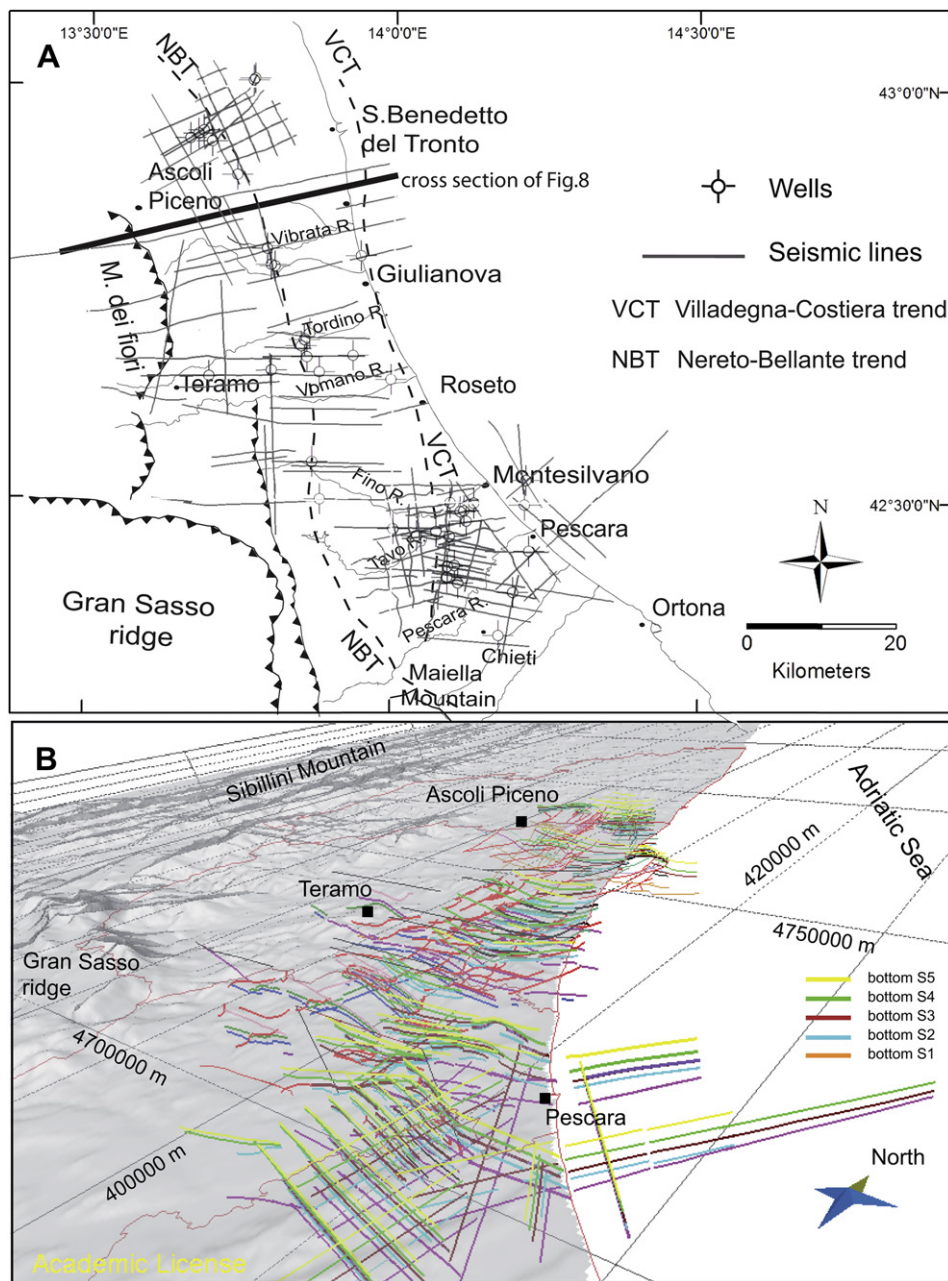


**Figure 2.** A) Basemap of the used dataset. The available well logs are about 30. All the 2D seismic lines (about 100) were used for the 3D reconstruction, following the procedure indicated in the text. B) A general figure with the total dataset used for the 3D model reconstruction. The colored lines represents the horizons recognized on each seismic line, corresponding to the sequences boundaries. (For interpretation of the references to colour in this figure legend, the reader is referred to the web version of this article.)

Tyrrhenian back-arc extension and by the synorogenic sedimentation in foredeep basins developed at the front of the chain (Doglioni et al., 1997; Carminati et al., 1998). Thrusts fronts propagated toward the foreland, involving progressively younger and easternmost foredeep deposits into the orogenic wedge, and, at the same time, gradually shifted the depocenters of both foredeep and wedge-top basins further to the east (Ori et al., 1986; Ricci Lucchi, 1986; Dattilo et al., 1999; Scisciani and Montefalcone, 2006; Crescenti et al., 2004; Artoni, 2007). The Periadriatic foredeep, which extends from the Po plain to the north to the Gulf of Taranto to the south, records the latest evolutionary stages of the Apennines chain. The study area consists of the Marche–Abruzzi sector of the Periadriatic foredeep from Ascoli Piceno to the north to Pescara river to the south, and it is characterized by a non homogeneous

stratigraphy, both in longitudinal and in transversal direction (Fig. 1).

A Meso–Cenozoic pelagic carbonate succession crops out in the Montagna dei Fiori–Montagnone ridge to the west, whereas the carbonate platform of the Gran Sasso–Morrone and the Maiella tectonic units crop out to the south (Bigi et al., 2009 and references therein). To the east of this tectonic lineaments, i.e. Montagna dei Fiori–Gran Sasso–Maiella thrust fronts, foredeep siliciclastic sequences, progressively younger moving toward the Adriatic sea, crop out. They corresponds to i) the Upper Messinian turbidites of the post-evaporitic Laga basin, belonging to the footwall of the Mt. Fiori thrust (Centamore et al., 1991a,b; Paltrinieri et al., 1982; Di Francesco et al., 2010); ii) the Lower Pliocene sandstones and clays belonging to the Cellino basin, in the footwall of the Laga–

Cellino thrust (Centamore et al., 1991a,b; Casnedi et al., 1976; Casnedi, 1983; Ori et al., 1991; Patacca et al., 2008; Bigi et al., 2011); iii) the Middle Pliocene–Pleistocene post-orogenic sequences deposited within the Periadriatic Basin (Ori et al., 1986; Carruba et al., 2006).

The definition of the main seismic sequences within these deposits constituted an important part of our study, that allowed to date the main deformation and uplift processes of this area and to quantify the deformation rates. These deposits crop out in an elongate, roughly north to south oriented narrow trough (some 200-km long and 30-km wide) generally gently dipping eastward, to form a regular wide monocline. They consist mostly of silt and clay with coarse grained strata at different stratigraphic position (Ori et al., 1991; Crescenti et al., 1980; Bigi et al., 1997; Artoni, 2007). The bottom and the top of these sequences are usually signed by the occurrence of conglomeratic-sandy neritic transgressive deposits. The Middle–Upper siliciclastic sequence cropping out in this sector of the Periadriatic basin can be considered a complete transgressive–regressive cycle, showing a deepening-upward trend during the Middle–Late Pliocene *p.p.* and a shallowing-upward trend during the Late Pliocene *p.p.* – Pleistocene. Afterward, a continental sedimentation occurred. Although it keeps the same evolutionary trend within all the basin, this succession shows many facies and thickness variations both horizontally and vertically, and strong angular unconformities, as a consequence of fold and thrusts propagation that, in the same time, was active in this area. Different depositional sequences can be recognized, bounded by unconformities in the inner parts of the basin, and by correlative conformities in the deepest and distal areas, where the depositional sequences show maximum thickness and continuity of sedimentation. This sequences are called P2, Qm, Qm1, Qc in Bigi et al. (1997) and references therein, and MP1, MP2, UP, Q in Ori et al. (1991), among the others.

The tectonic structures affecting the foredeep deposits during this time consist of eastward verging thrusts and related folds, trending roughly N–S. The Montagnone–Montagna dei Fiori Thrust overlaying the Lower Messinian foredeep deposits of the Laga Fm. and the pre-orogenic carbonate substratum on the upper part of the same Laga Fm. (Milli and Moscatelli, 2000). It is a splay of a regional, N–S thrust named Teramo thrust (Bigi et al., 2011 and references therein; Fig. 1). This main structure is buried under the Marne del Vomano Fm. (Lower Pliocene) to the north of the Vomano River, tectonically places the Messinian foredeep domain, largely cropping out to the west, onto the Lower Pliocene foredeep domain, consisting of the foreland meso–cenozoic carbonate succession and the Cellino Fm. (Lower Pliocene) at the top. To the south, the more eastern carbonate platform succession of Maiella anticline over thrusts the Lower Pliocene siliciclastic deposits, and is unconformably covered by the Upper Pliocene–Lower Pleistocene sediments of the Periadriatic basin.

Eastward of this sector of the chain, two buried thrust-related anticlines have been recognized from drilling and seismic-reflection datasets; they developed roughly NNW–SSE and subdivided the foredeep into two narrowed sectors showing different depositional settings: an internal wedge top basin, showing the shape of a wide, passively transported, syncline, and a more external and less deformed, wedge-shaped, foredeep basin (Ori and Friend, 1984; Flemings and Jordan, 1989; DeCelles and Giles, 1996; Ford, 2004).

The inner thrust-related anticline trend, named Nereto–Bellante Trend, delimited the piggy back basin to the west; it is formed by stacked thrust sheets involving meso–cenozoic carbonate and Messinian siliciclastic succession; the detachment level can be located within the Triassic evaporites (Bally et al., 1986; Ori et al., 1991; Bigi et al., 1997; Patacca et al., 2008).

The outer one, known as Costiera Structure Trend, delimited the piggy back basin to the east and divides the foredeep s.s from the undeformed foreland. The Costiera Structure formed an imbricate E-vergent thrust system, running parallel to the present day coast line; its sole thrust is located by the Authors in the Messinian evaporites or in the Cretaceous pelagic sequences (Bally et al., 1986; Ori et al., 1991; Artoni and Casero, 1997; Bolis et al., 2003; Casero, 2004).

### 3. Methods

In recent years, thanks to the development of increasingly sophisticated software, the classical two-dimensional view of geologic data, such as maps, cross sections, etc. was replaced by digital three dimensional representations. 3D modeling allows to detect and analyze complex spatial relationships, leading to a better characterization of both exposed and subsurface geology. It is especially useful in cases where the structures are not cylindrical, when 2D visualization could be not completely useful. The increasing ability of geological software packages to integrate and visualize different datasets in a 3D framework allows for a more critical evaluation and triggers a convergence of interpretations.

3D modeling involves different kind of data, so different methods can be developed. Here we present a model generated through the interpolation between closely and regularly spaced 2D seismic reflection profiles, integrated and calibrated with borehole data. The work has been carried out by means of a dataset, a geographic information system and a geo-modeler (Fig. 3).

The first step consisted into the collection, the selection and the revision of all the available data, such as geological maps, geological sections, isochrones maps, seismic profiles and borehole data.

The number of the available seismic profiles are one hundred (Videpi Project, 2009); besides of them, we also used several confidential seismic lines, especially in the northern part of the study area (Ascoli Piceno area). The data was subsequently processed in order to build a consistent dataset: seismic line basemaps, well position and geological maps were geo referenced in a common coordinate system (European Datum 50) and organized in a geographic information system in ArcGIS (Esri).

The geological maps and the isochrones maps were used mainly to define the general stratigraphic and structural framework of the area. The constraints obtained by this revision were taken into account during the well log correlation and then during the 3D reconstruction. Part of the seismic profiles were in raster format, so we produced .seg-y files for each raster seismic line in order to be able to import all the dataset into the interpretation software; this was achieved using image2seg-y 2.2.6, a free tool developed by the Instituto de Ciencias del Mar (Spain) for Matlab software, that allows to create a geo referenced seg-y file from a scanned seismic image.

A total of 1000 km of seismic lines and of 40 wells data were interpreted, together with the released well logs; exploration wells are concentrated along the two main structural trends, whereas less information is available in the other areas. As well as the boreholes, even the seismic lines distribution is variable; nevertheless the average spacing is about 4 km; where seismic lines are closer, we interpreted all the lines but used in the 3D modeling the best quality ones.

Once the dataset was complete and available, we proceeded to detect the angular unconformity surfaces and the correlative conformity surfaces on all seismic lines. We define the nature of reflectors terminations as well as the seismic amplitude, frequency, geometry of reflectors and of seismic units. Composite well logs data were used to calibrate the seismic lines, in order to give a chronostratigraphic constraint to the identified unconformities

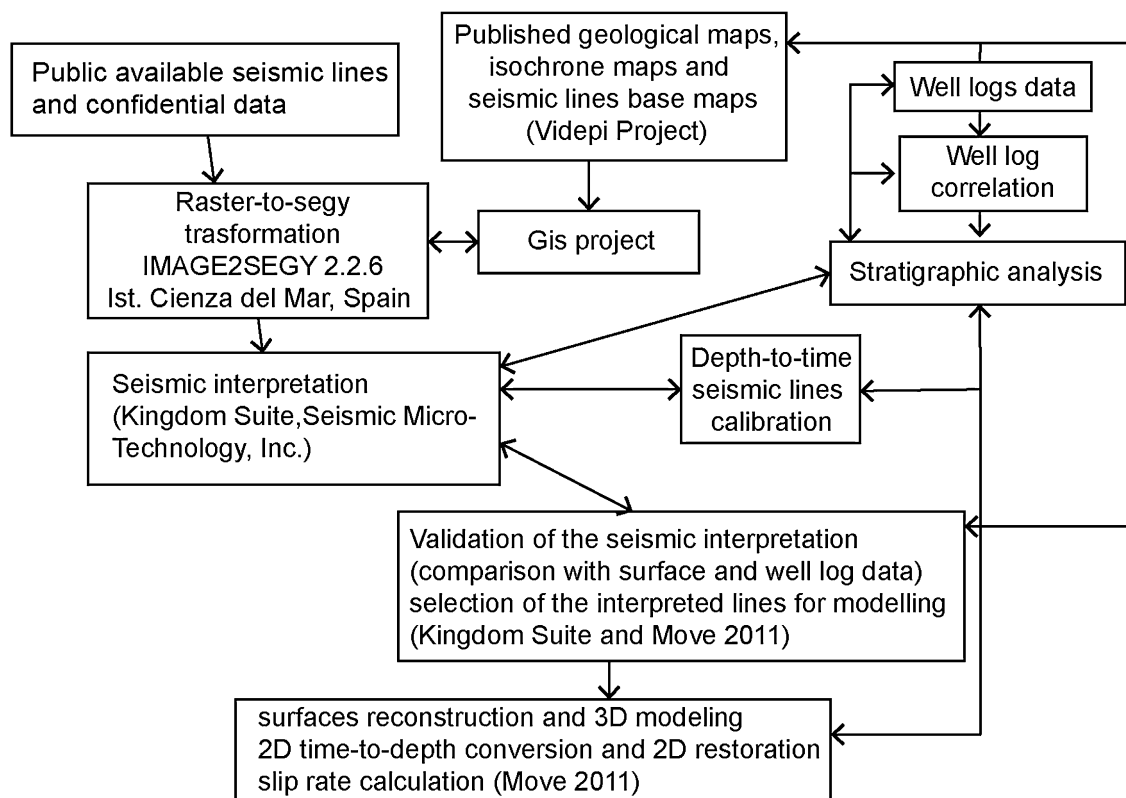


**Figure 3.** Flowchart adopted in this study. The first part of this workflow regards the preparation of the dataset (raster-to-segy conversion, well log analysis and correlation) that was the base for the seismic interpretation. The second part regards the building of the 3D model, restoration and slip rate calculation.

surfaces. Moreover, in few cases, velocity logs were available for a direct depth-to-time conversion; in the other cases average velocity obtained by the analysis of the available logs and from literature have been used.

Several unconformity-bound units were identified (called  $S_0$ ,  $S_1$ ,  $S_2$ ...), characterized by homogeneous lithology, stacking patterns and facies association. The sequences were defined in detail on best-quality seismic lines and then extended above all the basin by means of intersections between dip and strike seismic lines. Before the 3D reconstruction the seismic lines interpretation has been generalized and extended to all the selected seismic lines where all the defined sequence boundaries have been recognized and traced.

An export file including all the horizons identified was then created and the data imported in 3DMove 2011 (Midland Valley) (Figs. 2B and 4). This software enables geoscientists to create structural models and provides tools for structural restoration, validation and analysis. In this case, the “Create surface from points” toolbox was used to generate surfaces from the imported horizons.

Fault surfaces were first built, then stratigraphic horizons were created; the mesh quality depends on the regularity of the line sampling; the density of triangles within the created surface is a function of the point density in the original model. Line regularization can be a way to obtain a good mesh quality and the “resample” tool can be used for later improvement of the surface mesh.

Fault network divided the model into regions where stratigraphic horizons are continuous, so it is important to determine how faults terminate onto each other before considering other geological surfaces (Caumon et al., 2009). Then, horizons construction can be made in each region defined by the faults, paying attention that horizon borders are properly located onto

fault surfaces; an alternative option is to create first each horizon and then cut it by the faults. Several artifacts may arise during this operations, so manually re-drawing or editing can be needed.

The modeling in time has been made in order to avoid discrepancies among lines due to the time-to-depth conversion eventually applied to each section. The resulting model is potentially ready to be converted in depth using the available toolbox provided by Move 2011 (Midland Valley), that is likely the next step of the project. Moreover, performing the depth conversion on a total volume between two surfaces rather than on each section is a way to minimize the errors, because they result to be homogeneously redistribute on all the model.

#### 4. Seismic stratigraphy

Seismic lines unconformity-bound units reflecting significance changes at the scale of the whole basin were recognized and mapped. A detailed seismostratigraphic analysis of the Pliocene–Pleistocene deposits in terms of geometries and strata termination was carried out and six seismostratigraphic units ( $S_0$ ,  $S_1$ ,  $S_2$ ,  $S_3$ ,  $S_4$ ,  $S_5$ ) were defined. The defined units, each one characterized by an external geometry and an internal configuration (geometries of the reflectors, amplitude, frequency, etc), were then correlated across the seismic lines network and so reconstructed through all the basin. Next, by means of outcrop and biostratigraphic data and correlation with well-log stratigraphy, the seismic units were constrained from a chrono-lithostratigraphic point of view, the unconformity surfaces were linked to a chronostratigraphic scheme, and correlated to the seismic stratigraphy already published in this area (Fig. 5). So it was possible to divided the Plio–Pleistocene succession in units which represents different stages of the Periadriatic basin evolution.

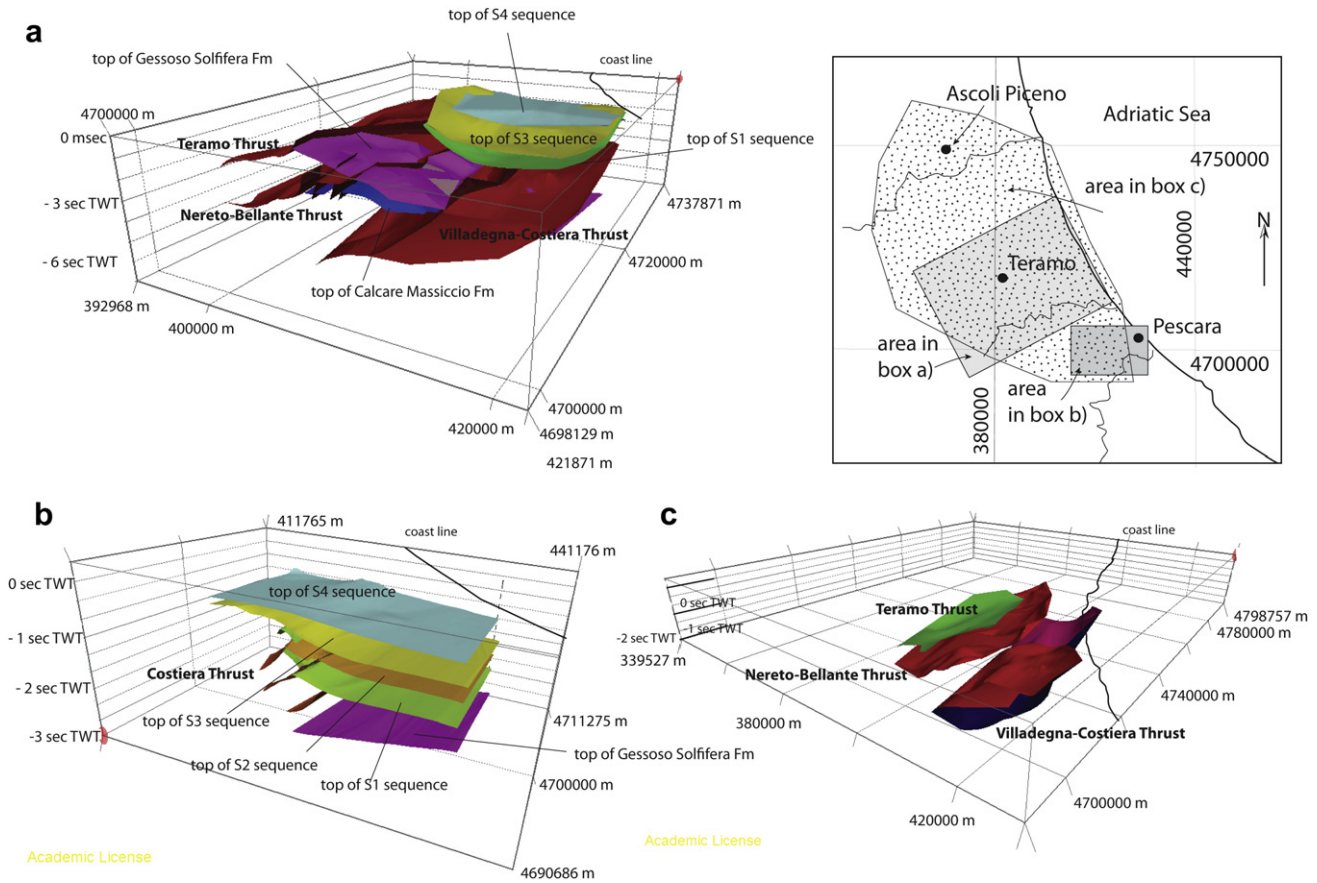


Figure 4. Some sectors of the 3D model of the study area. The areas covered by the different parts are defined in the map; the geological horizons corresponding to each surface are also indicated. In the box c) are represented the three surface corresponding to the three main thrust recognized in this area.

My	Series Epoch	Stage/Age							My	
			1	2	3	4	5	6		
0	Pleistocene	Upper						unit 8		0
1		Ionian		Gb. truncatulinoides excelsa	UPI	Q	?	S5		
		Calabrian		Gb. cariaeoensis			unit 7			
2	Pliocene	Upper	Gelasian	Gb. inflata	Gb. inflata	MP2	UP	unit 6	S4	2
3			Middle	Piacenzian	Gb. crassaformis			Gb. aemiliana	MPI2	MPI?
4	Lower	Zandean		Gb. crassaformis	Gb. aemiliana/seminulina	MPI1	LP2	unit 4		
			G. bononiensis	Gb. puncticulata	LPI5			LP1	unit 3	S1
5			Gb. puncticulata	Gb. puncticulata/Gb. margaritae		LPI4	M		unit 2	S0
			Gb. margaritae	Gb. margaritae	LPI3				unit 1	
6	Miocene	Messinian		S. seminulina s.l.		LPI2				
7							LPI1			

Figure 5. Chronostratigraphic table. Seismic sequences recognized in this work (6), compared with previous work (modified after Artoni, 2007). (1) Biozones of Crescenti et al. (1980); (2) Biozones of Iaccarino (1985); (3) Sequences of Crescenti et al. (2004); (4) Sequences of Ori et al. (1991); (5) Sequences of Artoni (2007). Numerical ages are from Grandstein et al. (2004) and from Ogg et al. (2008).

Hereafter we present the main seismic sequences recognized on our seismic dataset. The units were defined on those lines where geometries and chrono–lithostratigraphic correlation were more evident (Fig. 6); some difficulties were found in the definition of the deepest units due to the insufficient depth of wells. For example, is a matter of debate the occurrence of the Messinian deposits of the Laga Fm. under the recognized sequences, as well as the stratigraphy of the Paleogene and Mesozoic carbonate. These horizons has been traced on the internal seismic lines, calibrated to the available well logs and based on the interpretation of seismic dataset located more to the west (Bigi et al., 2011 and references therein); two examples of these lines are shown in Figure 7. Nevertheless, we focused our work on the Pliocene–Quaternary evolution of the basin.

#### 4.1. $S_0$ sequence

The lowermost sequence shows a basal unconformity formed by two high amplitude reflectors, offset by mainly east dipping normal faults. Using the well log “Fratello 1”, located in the Abruzzi offshore, this reflectors were interpreted as constituted by the primary evaporites of the Gessoso Solifera Formation (Videpi Project, 2009). The upper unconformity is a surface tilted eastward, with reflector’s terminations from top lap to parallel. The seismic sequence is formed by parallel and continuous reflectors,

showing variable thickness from north to south; east of the Costiera structure the unit shows the minimum thickness, as a lateral pinch out against the foreland ramp occurs. Sequence  $S_0$  is of difficult interpretation, as few well logs reaches such depths; however, seismic facies are recognized as sandstone and clay of turbiditic deposits, and the unit has been correlated with the Cellino Formation and the lowermost “Argille a *Sphaeroidinellopsis*” (Bigi et al., 1997; Vezzani et al., 2010). It comprises (includes) the *Sphaeroidinellopsis* zone (lower Early Pliocene) to the *G. punctulata p.p* zone of Crescenti et al. (1980) and/or *G. margaritae*–*G. punctulata* zone of Iaccarino (1985) (upper part of Early Pliocene). To the east of the Costiera anticline the sequence is thinner and the seismic facies is recognizable as distal turbiditic deposits; it is difficult to define whether the all the biostratigraphic zone is represented in this succession, because no well logs in this area are available. This unit can be correlated with Unit 1 and Unit 2 of Artoni (2007). It shows a very variable thickness, from about 1.5 s TWT in the internal syncline up to 0.5 s TWT to the east of the Costiera Structure (line C of Fig. 6; Line E of Fig. 7).

#### 4.2. $S_1$ sequence

The basal unconformity of the  $S_1$  sequence, to the east of the inner trend is a surface dipping westward, characterized by the eastern onlap of the reflectors in the lower portion of the same sequence; the

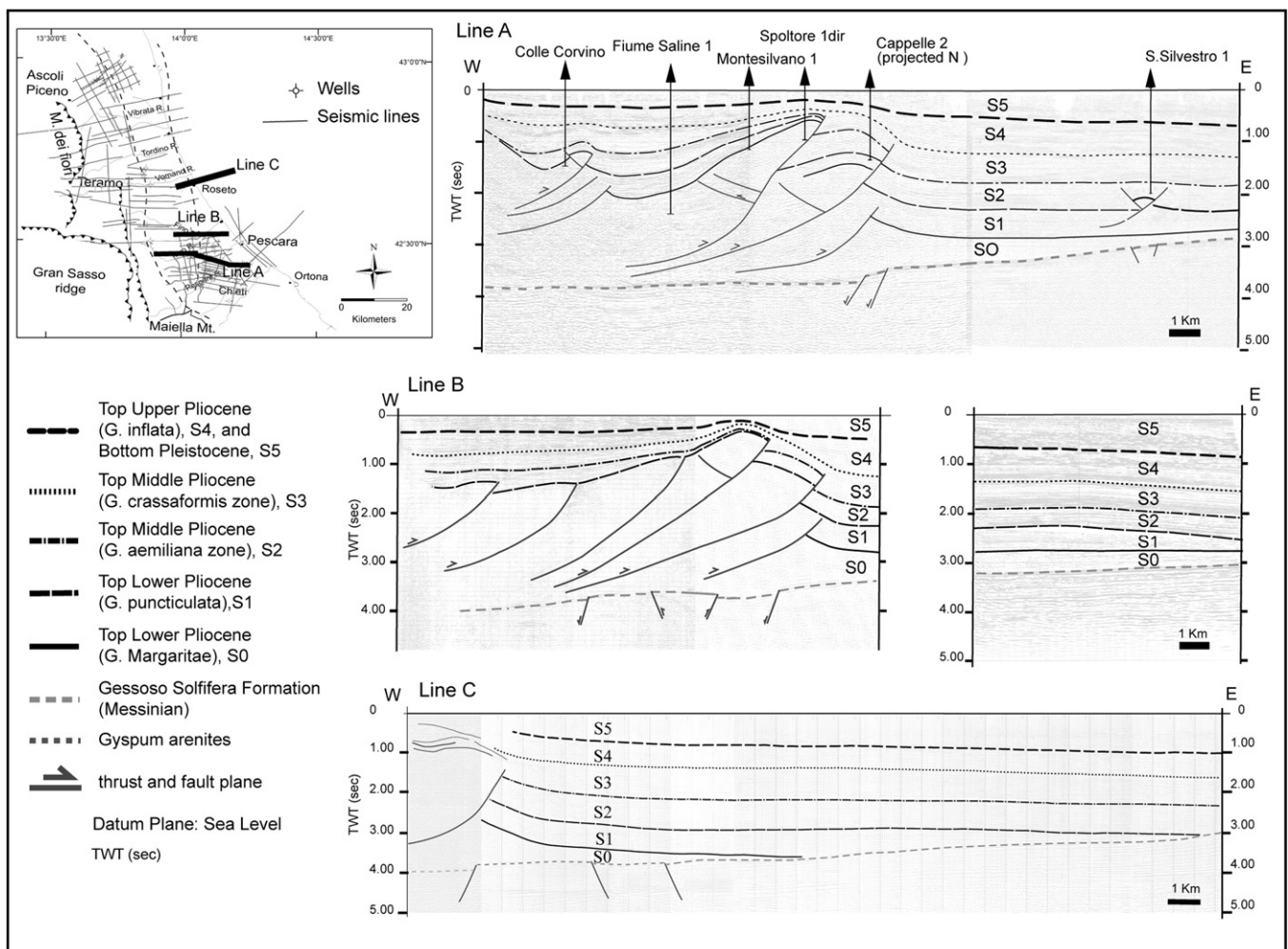


**Figure 6.** Seismic sequences recognized in the area, evidenced in three seismic lines from different part of the basin. The complex structure of the Costiera thrust is also evidenced. Note the break back sequence of deformation that can be reconstruct at the crest of the anticline.

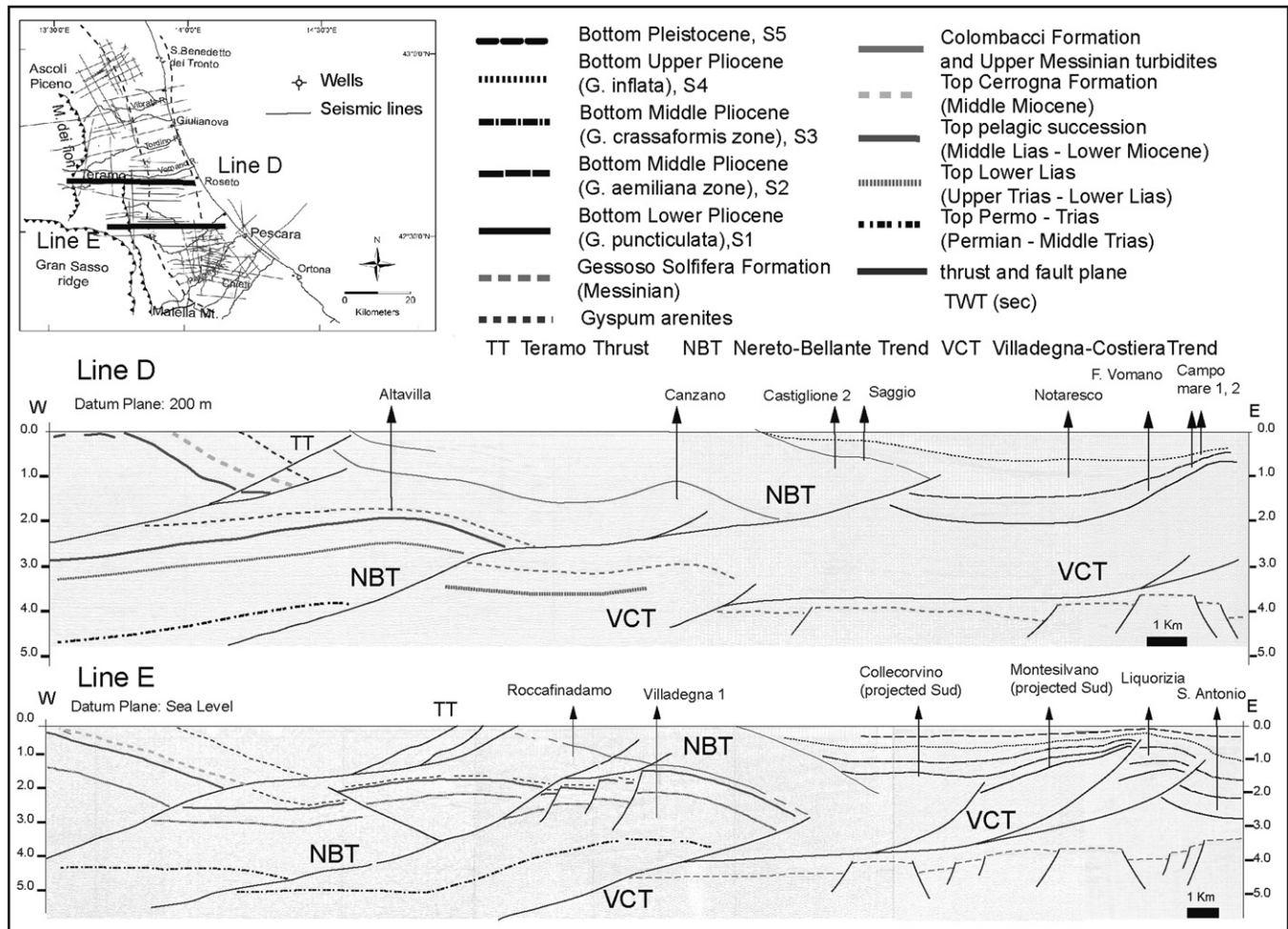


**Figure 7.** Interpreted seismic sections representative of the relationship between the Nereto–Bellante and the Villadegna–Costiera thrust systems in the central and in the southern sectors of the basin.

upper boundary is also dipping to the west, so the resulting external geometry is a wedge, gently concave to the top. In some sectors, close to the Costiera structure, it seems truncated by the lower boundary of the younger sequence (bottom of  $S_2$ ) (line B, Fig. 6).

This unit is thicker westward, where the reflectors have a growing fan shape progressively cut by a thrust, and thinner eastward, where the lateral termination is an onlap onto the lower boundary surface. The seismic facies is characterized by internal reflectors showing high amplitudes and good lateral continuity, mainly in the western part; closer to the Costiera structure, to the east, these characters are less evident. In the footwall of the Costiera thrust, this sequence shows a planar geometry; seismic reflectors are parallel, laterally continuous and sub-horizontal (line C, Fig. 6). The thickness reaches about 0.6 s TWT in the syncline and offshore, whereas tends to zero on the top of the Costiera anticline. This sequence can be referred to the upper part of the *G. punctulata* zone of Crescenti et al. (1980) or to the *G. punctulata* zone of Iaccarino (1985), due to the occurrence of *G. bononiensis* in the shales close to the upper boundary of the unit (Ori et al., 1991). The basal boundary corresponds to the Montefino unit of Casnedi et al. (1976), as confirmed by correlation with the outcropping geology (Vezzani et al., 2010).

The  $S_1$  unit marks the initial onset of the development of both the internal and the external ridges; it is poorer of clastic material than  $S_0$  sequence, and consists of turbiditic systems generally less mature. The  $S_1$  sequence can be correlated to the Unit 3 of Artioni

(2007), or to the LPI5 of Crescenti et al. (2004) and to part of the LP2 of Ori et al. (1991).

#### 4.3. $S_2$ sequence

The lower boundary of this sequence in the internal sector of the basin is marked at the base by the concave surface at the top of  $S_1$ , previously described. On this unconformity surface, the internal reflectors progressively onlap. The upper boundary is also an angular unconformity tilted to the west, parallel to the internal reflectors.

The internal reflectors are continuous and characterized by medium amplitude. They show a thickness reduction toward the Costiera structure. The  $S_2$  is strongly wedge shaped, with the maximum thickness (about 0.5 s TWT) corresponding to the back limb of the syncline and the minimum thickness over the crest of the Costiera anticline, where the termination of the reflectors is an onlap. On the hinge zone the truncation due to the upper unconformity can be observed. To the east of the forelimb of the Costiera anticline, the upper boundary unconformities passes to a conformable surface and the thickness progressively decrease very slowly eastward, due to the onlap of the lower reflectors on the lower boundary surface. Here the internal reflectors are sub-horizontal, parallel, with strong amplitude and laterally continuous, whereas in the upper part they show minor amplitudes and continuity (line C, Fig. 6).

The seismic facies highlights the occurrence of pelitic deposits with conglomeratic and sandy bodies located at different stratigraphic levels. We correlate these bodies to the channeled conglomerates, sheet conglomerates, sheet sandstones or channel–levee complexes of Ori et al. (1991). By means of well correlation, the lower boundary was ascribed to the *G. aemiliana* (Middle Pliocene) and the upper boundary to *G. crassaformis* (Middle Pliocene). This sequence is equivalent to the LP2 sequence of Ori et al. (1991), the MPI1 sequence of Crescenti et al. (2004) and to the Unit 4 of Artoni (2007).

In the seismic lines located offshore immediately below the upper unconformity is visible a chaotic seismic facies with indistinct and disorganized reflectors; this interval could be related to an episode of sedimentation of gravitative origin; the unconformity that bounds this group of reflectors at the top is an erosional, diffractive surface.

#### 4.4. $S_3$ sequence

This unit is similar to the previous one ( $S_2$ ). In the internal syncline, it shows a wedge shape geometry, with its maximum thickness close to the west and the onlap termination on the lower unconformity surface (about 0.6 s TWT); thickness is minimum on the hinge of the Costiera anticline. The pinch out on the back limb of the anticline decreases progressively upward, and the sequence has a smooth closure to the east. To the east of the Costiera structure, both the lower and upper boundaries are conformable surfaces; here has a thickness of about 1 s TWT, that is progressively thinner eastward.

The lower boundary is referred, as already said, to the *G. crassaformis* zone of the Middle Pliocene; the upper boundary is referred to the bottom of the *G. inflata*, at the base of Late Pliocene. The seismic facies is similar to the sequence  $S_2$ , with parallel horizons, low amplitude and high frequency in the central part of the syncline, indicating conglomeratic and sandy bodies; the limbs of the anticlines are characterized by clayey-marls with interbedded conglomeratic lenses at different stratigraphic levels, referred to channelized fan systems (Ori et al., 1991). A general trend during Middle Pliocene is the decreasing of the amount of clastic supply toward the top of the sequence.  $S_3$  sequence can be correlated to the Unit 5 of Artoni (2007), to the MPI2 sequence of Crescenti et al. (2004) and to part of the MP1 and MP2 sequence of Ori et al. (1991).

#### 4.5. $S_4$ sequence

The lower unconformity of  $S_4$  sequence is gently tilted westward, whereas the upper boundary is sub-horizontal; this unit has a lens shape, thinning both westward and eastward, toward the Costiera anticline. Internal reflectors are parallel and sub-horizontal, continuous and with medium amplitude; they evidence a growth geometry on both the limbs of the Costiera anticline. Toward the foreland the unit boundaries are correlative conformities. The thickness varies from 1.2 s TWT to about 0.2 s TWT. More in detail, the basal boundary can be clearly identified on seismic lines because it corresponds to a volcanoclastic level dating Late Pliocene (Pironon and Champanhet, 1992).

$S_4$  sequence bypasses the hinge of the Costiera Structure (line A of Fig. 6); the basal unconformity is referred to the *G. inflata* zone, whereas the upper boundary is dated to the base of Pleistocene (*G. cariacensis* and *G. truncatulinoides excelsa* according to Iaccarino, 1985). This sequence, located within the *G. inflata* zone, corresponds to the upper part of MP2 sequence of Ori et al. (1991), to the Unit 6 of Artoni (2007) and to UPI of Crescenti et al. (2004). According to Ori et al. (1991),  $S_4$  sequence has less coarse grained

basal deposits; close to the Costiera structure, it consists of fore-shore and shoreface deposits, whereas, to the east, it is made of channeled and than basinal deposits. The occurrence of shoreface systems suggests shallow water conditions.

#### 4.6. $S_5$ sequence

The most recent unit,  $S_5$ , has a tabular geometry, with the basal unconformity dated to the base of Pleistocene. Internal reflectors are parallel and continuous, from sub-horizontal to gently tilted eastward; this sequence bypasses the Costiera structure and seals it (Figs. 6 and 7). The sequence thickness increases toward the foreland; eastward progradation and the occurrence of clinofolds with sigmoidal reflectors are clearly visible on seismic lines located offshore (line C of Fig. 6) This unit can be correlated to unit 7 and 8 of Artoni (2007), UP and Q of Ori et al. (1991), and is characterized by continental/shallow marine coastal facies, passing eastward to mound turbidites (Ori et al., 1991).

### 5. The structural setting of the area from the 3D model

The 3D model is based on the interpretation of several key horizons on 2D seismic lines, constrained with well logs and surface geology (Figs. 2 and 3). It allows to reconstruct the main geological surfaces in the Central Periadriatic basin and to define the relationship among the main recognized geological structures (Fig. 4).

The main structural setting comprises structural trends roughly N–S, involving the meso–cenozoic carbonate succession and buried under the Plio–Pleistocene sequences; in the western portion of the basin, close to the outcropping thrust front of the chain corresponding to the Teramo thrust (Bigi et al., 2011 and reference therein), the internal trend results to be composed by two tectonic units characterized by different structural elevation to the north and to the south of the basin: the Nereto–Bellante thrust to the north and the Villadegna thrust to the south (Fig. 7). Eastward, along the present coast line, the external trend is constituted by the Costiera thrust related anticline; this thrust plane is structural connected with the Villadegna–Costiera Thrust. These two main trends subdivided the basin in two depocenters: the inner one, which shows the shape of wide syncline, bounded to the west by the Nereto–Bellante thrust and the Villadegna–Costiera Thrust to the east; the outer one, between the Costiera Thrust and the Adriatic offshore where the sequences have a wedge shape corresponding to the foredeep basin monocline (Fig. 4).

Thrust trajectories are generally the same for all the structural unit and are characterized by deeper high angle ramps located in the carbonate sequence followed by long flats at the top of the same carbonate succession and shallower ramps and related anticlines involving the Plio–Pleistocene siliciclastic sequence. The first, deeper ramp is connected to the development of the internal trend (Nereto–Bellante thrust and Villadegna–Costiera Thrust), whereas the second ramp controls the external anticline (Costiera Thrust). The 3D reconstruction allowed us to correlate these main trends along strike, revealing a variation in the geometric relationships, in the displacement and in the chronology of deformation.

#### 5.1. The Nereto–Bellante structure

The Nereto–Bellante structure, is characterized by a staircase geometry evolving toward the south to a single thrust ramp (Figs. 4 and 7). In the southern sector, this ramp cut through the carbonate succession and has a small displacement along the thrust plane, as well as the upper flat. The basal detachment is located at 4.5 s TWT, and the thrust is covered by the Lower Pliocene deposits, that crops

out in this area. To the north, the lower ramp still offsets the carbonate pelagic succession whereas the upper ramp progressively affects the siliciclastic deposits of the Upper Messinian and Lower Pliocene. The frontal zone is quite complex and composed by several splays with a short continuity along strike; each splay from the main thrust plane is associated to a hanging wall anticline (Fig. 7). In the northern sector, a wide anticline develops in the hanging wall of the splays system; on its forelimb the synkinematics Pliocene deposits onlap progressively (Figs. 4, 6 and 7).

Between the Pescara river and Teramo city, the main direction is N–S, the anticlines keep a constant structural elevation, and the crest of the anticlines, corresponding to the top of the pre-orogenic sequence, located at 1.5–2 s TWT. To the north of Teramo city, the main direction is N 30°W, whereas to the south, the direction is mainly N10°–20°E (Figs. 1 and 4).

In the southern sector, to the south of the Pescara river, the Nereto–Bellante thrust ramp cut through the carbonate succession and has a small displacement, as well as the upper flat (Figs. 4 and 7). The basal detachment is located at 4.5 s TWT, and the thrust is covered by the Lower Pliocene deposits, that crops out in this area (Figs. 1 and 7). To the north, the lower ramp still offsets the carbonate pelagic succession whereas the upper ramp progressively affects the siliciclastic deposits of the Upper Messinian and Lower Pliocene. The Nereto–Bellante trend has in this sector an upper flat that links these fronts to the lower ramp crossing the carbonate sequences; this flat is located at about 3.5 s TWT, whereas the basal detachment is located at about 6 s TWT (Fig. 7).

### 5.2. The Villadegna–Costiera thrust

The Villadegna–Costiera structure is the lowest tectonic feature in the studied sector; its surface is characterized by a staircase profile showing an axial plunge toward the north, where it is barely visible in the seismic lines underneath the NBS thrust front. The forelimb of Villadegna anticline is characterized by an active axial surface involving the synorogenic Lower Pliocene Cellino deposits. Later the axial surface became inactive as shown by the Lower Pliocene–Lower Pleistocene final onlap on the anticline forelimb, corresponding to the *G. Puncticulata* Zone. The Villadegna–Costiera thrust has a trajectory composed by two main ramp connected by a long flat developed at the top of the carbonate sequence. In the southern sector the lower ramp cuts the meso–cenozoic carbonate sequences, involved in the hanging wall anticlines. This latter progressively increases its structural elevation and more southward corresponds to the outcropping anticline of the Maiella Mountain. The plunging to the north is well define in the 3D reconstruction of the area (Fig. 4). In the northern sector, to the north of Vomano river, the same lower thrust ramp has a smaller displacement. The Villadegna–Costiera basal detachment is generally located at 6 s TWT. The branch line of the deeper ramp is located vertically under the Nereto–Bellante structure thrust front. The upper flat is located immediately above the Gessoso Solfifera Formation and is sub-parallel to the passively transported wide syncline filled by the syn- and post-orogenic deposits; it also connects the upper ramp of the Costiera Structure (Fig. 7).

The location of the branch point of the upper flat, connected to the Costiera thrust-related anticline development, generally corresponds to an area where the top of the carbonate succession and the Gessoso Solfifera Formation are offset by a number of mainly west-dipping small normal faults (Figs. 6–8). This correspondence is quite common along all the basins. The reconstruction of the Structure Costiera along strike from Ascoli Piceno to Pescara highlights this growing structure has different structural setting from south to the north. To the south, where the internal structure of Villadegna reaches the maximum structural level, the Costiera

structure is quite complex. It is composed by least three E-vergent thrust ramps and related anticlines, which result to be superimposed. Some back thrust are visible and a northern culmination is observed in the seismic lines. Following the same structure northward, the thrust ramps progressively reduced their offset and the whole structure becomes simpler. In the northern sector, close to Ascoli Piceno the Costiera Structure is located onshore and is composed by a simple ramp related anticline (Figs. 1 and 8). Moreover, in this area, the thrust trajectory is simpler even at depth, where the intermediate flat is poorly developed as well as the deeper anticline involving the carbonate succession (Fig. 8).

A foreland monocline is imaged by the seismic lines to the east and south of the Costiera anticline, in the Adriatic offshore. Here, a thick pile of Pliocene–Pleistocene strata onlap onto a gently westward dipping reflector corresponding to the top of the Gessoso Solfifera Fm. and offset by mainly westward dipping normal faults. This foreland monocline delimits seaward the basin delineated by the development of the Costiera structure and filled by the Middle–Upper Pliocene deposits (Fig. 8).

### 5.3. Displacements distribution and deformation chronology

The occurrence in the study area of a syn- and post-orogenic successions allowed the reconstruction of the thrusts activity and of the deformation chronology.

The reconstructed surfaces of the synorogenic deposits to the west of the Nereto–Bellante Structure show that this front acts as a single system during the Upper Messinian–Lower Pliocene, whereas the frontal thrust shows a main activity from the *G. Puncticulata* Zone until the *G. Inflata* Zone, which are the first undeformed deposits. In the southern sector the Nereto–Bellante thrust is older than in the north. Here the younger deposits involved in the deformation are dated at the Middle Pliocene, along the frontal thrust (Fig. 6).

The Villadegna–Costiera Structure was active from the *G. margaritae*–*G. puncticulata* Zones, and continued propagating forward and forming the Costiera anticline during the Lower–Middle Pliocene. More in detail, the activity of the Costiera anticline started during the upper part of Early Pliocene (*G. bononiensis* zone) whereas the end is progressively younger toward the North: in the southern seismic lines the thrust activity associated to the Costiera Structure offsets the base of Middle Pliocene (*G. crassaformis*), whereas moving to the North the basal unconformity of the Upper Pliocene is still offset, suggesting that the final activity is postponed until the Late Pliocene (Fig. 6).

Moreover, in the southern sector, where the Costiera Structure is composed by more than one splay, the relationship to the syn and post-orogenic sequence allows to reconstruct the sequence of deformation within the same structure (Fig. 6). Based on the offset chronology of the several boundary sequence, is possible to highlight that the internal sequence of deformation is a break-back sequence, where the more external thrust is the older one whereas the younger ones developed progressively in its hanging wall, cutting the developing anticline. This deformation sequence implies the development of an irregular shape of the anticline and the occurrence of small growing sequences on the hinge zone as observable in some seismic lines.

## 6. Geological section, depth conversion and restoration

In order to provide quantitative constraints based on our 3D model, reconstructed in time through the Periadriatic basin, one geological cross section has been chosen, converted from time to depth and restored. The cross section showed in Figure 8 is located

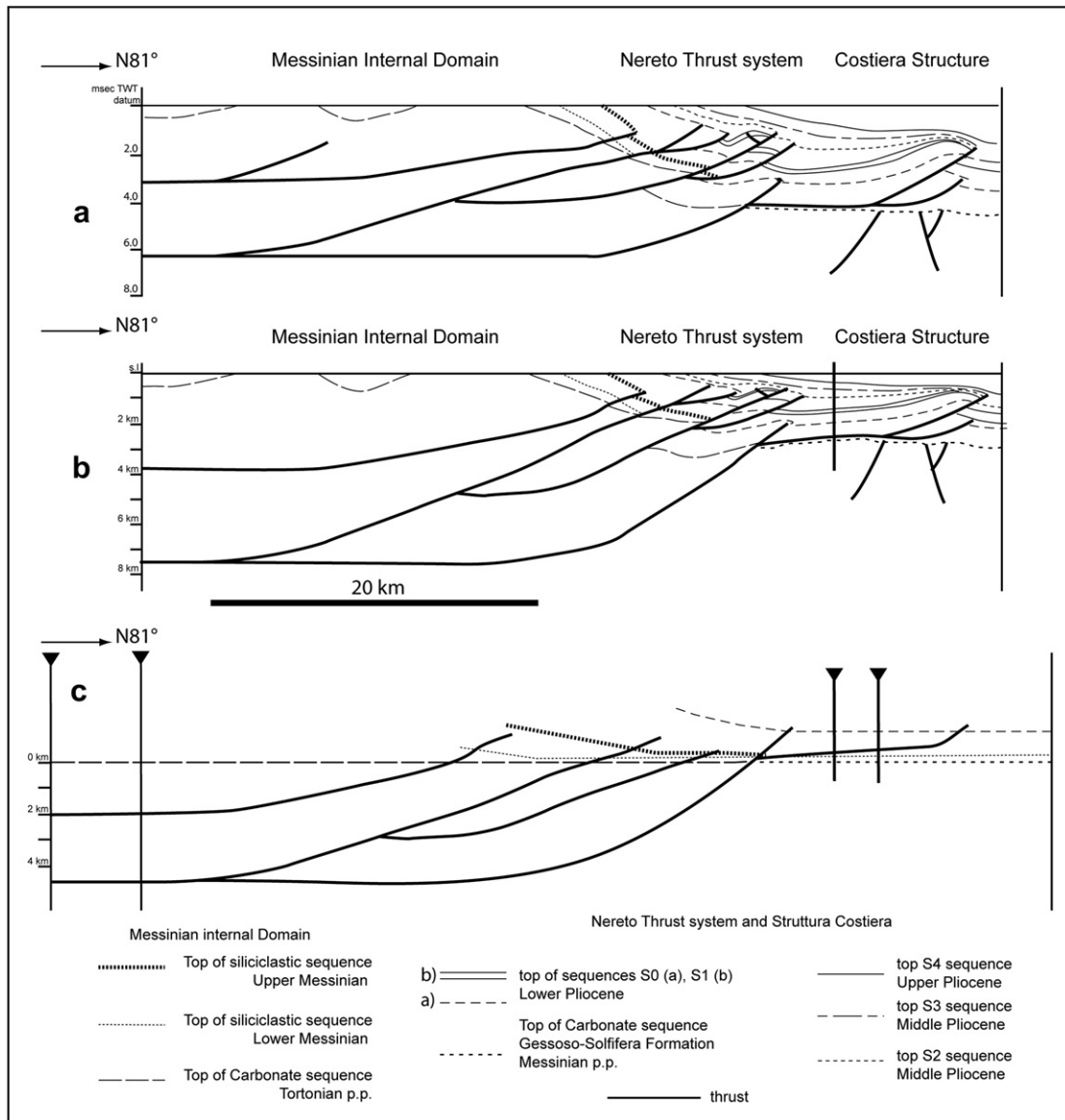


**Figure 8.** a) Interpreted seismic cross section in time through the northern sector (see Fig. 2A for location). b) time-to-depth converted section, according to the data of Table 1; c) restored section. Restoration was performed using Move 2011 (Midland Valley).

immediately to the south of Ascoli Piceno, in the northern sector of the basin, and crosses all the described structures.

The time-to-depth conversion was based on the velocity logs data available in the area (provided by Videpi and by other confidential data) and has been performed using the software Move 2011 (Midland Valley). The procedure was to assign an average velocity value to different areas of the section. The used average velocity values are listed in Table 1. The resulting section has been restored in several steps, from the more internal to the more external ones, following the constraints provided by the observation obtained from seismic interpretation and from the 3D model, and already treated. The restoring procedure was organized dividing the section into two main sections: an eastern segment and a western one, putting a pin line corresponding to the flat onto the Gessoso Solfifera Fm (see Fig. 8). The restoration of each thrust-related anticline included two steps: a) the restoration of the displacement along each fault plane and b) the unfolding of the hanging wall anticline. We ignored the flexural response to loading, although it is an important factor in this technique (Royden, 1988).

The restoration is limited to the Pliocene deformation, recorded by the pre- and syn-deformation deposits. The Pliocene flexure, represented by the angle between the Lower Pliocene horizons and the top of the Gessoso Solfifera Formation (see line C of Fig. 6) is not taken into account. The angular unconformities onto the limbs of the anticlines are considered as due to the local control exerted by thrust activity on sedimentation, as already demonstrated by forward modeling in the Po Plain (Zoetemeijer et al., 1992). Moreover, Messinian deformation is included only in the unfolding process of the top of the carbonate successions in the westernmost sector of the section (indicated as the Messinian Internal Domain), whereas the unflexed basement is represented by the east-dipping attitude of the Messinian horizon in the restored section (c in Fig. 8). The obtained total shortening is about 13% corresponding to 6 km on a section of 52 km of length (Fig. 8).

On the balanced and restored geological cross section the basal detachment of the wedge results to be located at about 8 km, closer to the ramp of Nereto and Villadegna structures and is progressively shallower eastward where the upper flat is at 4 km of depth.

**Table 1**

Velocity values used in the time-to-depth conversion of the section of Figure 8. The column Polygon (age) is referred to the name of the polygon drawn onto the section and corresponding to the different stratigraphic units. The third column indicates the location of each area (polygon) in the section (that required the use of different seismic velocities): (0) generic position; (1) footwall of Costiera thrust and foredeep; (2) top anticline; (3) internal syncline; (4) hanging wall of Nereto–Bellante thrust.

Polygon name (age)	Velocity (m/s)	Polygon localization
Pleistocene	2000.00	4
Upper Pliocene ( <i>G. inflata</i> )	2200.00	0
Upper Pliocene ( <i>G. inflata</i> )	2100.00	1
Upper Pliocene ( <i>G. inflata</i> )	2200.00	2
Upper Pliocene ( <i>G. inflata</i> )	2100.00	3
Upper Pliocene ( <i>G. inflata</i> )	2200.00	4
Middle Pliocene ( <i>G. aemiliana</i> )	2400.00	1
Middle Pliocene ( <i>G. aemiliana</i> )	2500.00	0
Middle Pliocene ( <i>G. aemiliana</i> )	2500.00	2
Middle Pliocene ( <i>G. aemiliana</i> )	2400.00	3
Middle Pliocene ( <i>G. aemiliana</i> )	2500.00	4
Middle Pliocene ( <i>G. crassaformis</i> )	2400.00	1
Middle Pliocene ( <i>G. crassaformis</i> )	2500.00	0
Middle Pliocene ( <i>G. crassaformis</i> )	2500.00	2
Middle Pliocene ( <i>G. crassaformis</i> )	2400.00	3
Middle Pliocene ( <i>G. crassaformis</i> )	2500.00	4
Lower Pliocene (undefined)	2800.00	0
Lower Pliocene (undefined)	2700.00	1
Lower Pliocene (undefined)	2800.00	0
Lower Pliocene ( <i>G. puncticulata</i> )	2800.00	3
Lower Pliocene ( <i>G. puncticulata</i> )	3000.00	4
Lower Pliocene ( <i>G. puncticulata</i> )	3000.00	2
Lower Pliocene ( <i>G. bononiensis</i> )	2600.00	1
Lower Pliocene ( <i>G. bononiensis</i> )	2600.00	3
Lower Pliocene ( <i>G. bononiensis</i> )	2600.00	0
Lower Pliocene ( <i>G. bononiensis</i> )	2700.00	4
Lower Pliocene ( <i>G. bononiensis</i> )	2700.00	2
Lower Pliocene ( <i>G. margaritae</i> )	2800.00	3
Lower Pliocene ( <i>G. margaritae</i> )	3000.00	4
Lower Pliocene ( <i>G. margaritae</i> )	3000.00	2
Pliocene (undefined)	2800.00	0
Pre-evaporitic succession	3200.00	0
Colombacci Formation	3100.00	0
carbonates Apulian platform	5000.00	2
carbonates Apulian platform	4500.00	1
Carbonate succession	5100.00	3
Carbonate succession	5000.00	2
Carbonate succession	5000.00	0

The Nereto–Bellante structure is here composed by at least two planes and by several splays in the more superficial part; their tectonic activity is documented in this section until the lower part of the Upper Pliocene (*G. inflata* Zone). Instead of the largely developed Nereto–Bellante thrust system, the Villadegna–Costiera thrust system is represented by the Costiera thrust related anticline here composed by a very simple growing structure. The lower ramp of the same system has a dip of about 40°, and a main direction of 20°W (Fig. 4, line D in Fig. 7, and Fig. 8). In this northern sector the offset connected to this thrust is small, as can be observed on the section at the structural level of the top of the carbonate succession. For the Costiera Structure, the detachment consists of the upper flat of the thrust system, connected to the Villadegna ramp, and is located between 2 and 3 km, on the top of the carbonate sequences referred to the Adriatic plate. The top of the Adriatic plate is offset by pre-Pliocene normal faults that could be reactivated as thrust plane in a compressive stress field.

The clear relationship between the growing anticline of the Costiera Structure and the overlapping sequences on the two limbs of the anticline, allowed the calculation of the slip rate and of the uplift rate of this structure, using a progressive restoration based on the restoration of each syn-deformation sedimentary sequence (Fig. 9). The restoration has been performed steps by steps using Move 2011 (Midland Valley). The procedure provided for each

seismic sequence, the following steps: a) flattening of the younger horizon; b) removing the offset along the fault of the restoring horizon; c) flattening of the obtained horizon. The obtained values, calculated using the equation proposed by Suppe et al. (1992), are resumed in Table 2, are in the range of growing rates of most of the anticline measured in different part of the world (Medwedeff, 1992; Suppe et al., 1992; Keller et al., 2012 and references therein). These values show a progressive reduction from Middle Pliocene up to now (Table 2 and Fig. 9). As is possible to observe by the comparison between the slip and the uplift rates, the slip rate results to be always lower than the uplift rate suggesting that the growth of the anticline is an active deformation mechanisms in the evolution of the Costiera anticline. Only during the deposition of the  $S_1$  sequence, the slip rate is higher than the uplift; this moment represent the time of the onset of the propagation of thrusting involving the Lower Pliocene foredeep deposits of  $S_0$  sequence. Moreover, the progressive rotation of the horizons as well as of the thrust trace during the flattening confirms a strong control of the anticline growth on sedimentation, except for the  $S_1$  interval.

## 7. Discussion

The 3D reconstruction of the structural setting in the Periadriatic basin between Ascoli Piceno to the north and the Pescara River to the south, allows to highlight several peculiar features of this sector of the Apennines chain. Generally, in the Periadriatic basin, the contractional deformation affected mainly the Pliocene–Pleistocene siliciclastic cover, where several syn- and post-orogenic sedimentary sequences can be recognized (Suppe et al., 1992; Poblet and Lisle, 2011). Thrusts and related folds propagating across the Meso–Cenozoic succession are connected to a shallow detachment level at the top of the carbonate substratum (located at depth of about 4 km below sea level). The lower and upper thrusts acted simultaneously and the compressive deformation migrated toward the ENE. The orogenic contraction was transferred from the inner and deeper levels toward the shallower detachment levels in the foreland; at the shallower level, the shortening was partitioned in a multiple array of thrust ramps and related anticline (Bigi et al., 2004; Tozer et al., 2006; Scisciani and Montefalcone, 2006; Bigi et al., 2011). Although the two main thrust systems recognized in this work, the Nereto–Bellante and the Villadegna–Costiera thrust systems have both this geometric organization, at a smaller scale the internal organization is quite different from north to south. This variation is strictly connected to the displacement distribution and the deformation chronology and our results suggest that these two main front, during their development, influenced each other their internal structure. Fault interactions has a broadly influence on the relationships that the individual faults may have with each other in balancing displacement. The difference of their internal geometry is the main reason why the internal trend is generally considered as a just one thrust system, where, instead, it results to be composed by two, complex systems that overlap along strike. Only their 3D reconstruction and the possibility to follow them through the basin enables to correlate the main thrust related folds along strike, and to highlight, in this way, their lateral continuity and/or their progressive reduction. Infact the wide time interval of common activity of the main thrust front does not help to reconstruct the continuity, because more than one thrust front is active at the same time, and in some cases, the occurrence of a break back sequence of deformation make the interpretation even more difficult.

In the northern sector the more developed structure is the structurally highest Nereto–Bellante thrust system, that shows numerous splays in the shallower zone (Figs. 7 and 8), whereas, in the south it is completely substituted by the Villadegna structure,

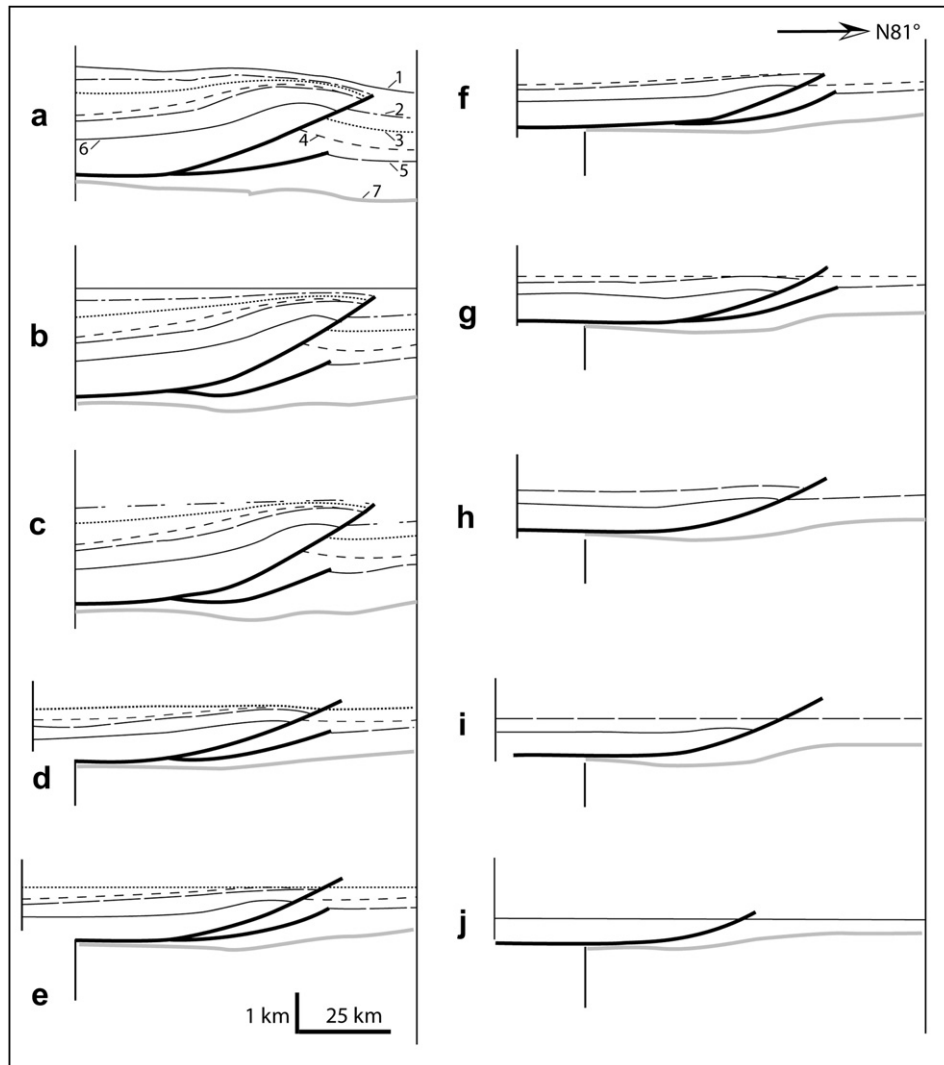


**Figure 9.** Restoration by steps of the Costiera Structure. The figure illustrates the three step applied to each horizon: a) flattening of the younger horizon (section b), e), g) and i); b) removing the offset along the fault of the horizon (section, d) and g) followed by a new flattening. 1) bottom of the Pleistocene ( $S_5$  sequence) and top of  $S_4$  sequence (Upper Pliocene); 2) Top of  $S_3$  sequence (Middle Pliocene); 3) top of  $S_2$  sequence (Middle Pliocene); 4) top of  $S_1$  sequence (Lower Pliocene); 5) top of  $S_0$  sequence (Lower Pliocene); 6) horizon within the  $S_0$  sequence; 7) top of the Gessoso Solifera Formation (Messinian).

that reaches the surface in the Maiella anticline. This interaction between these two thrust fronts is the results of several peculiar aspects of the fault activity, as the effective normal stresses acting on faults due to uplift, erosion, sedimentation and fluid pressure, that controlled the geometry of the chain at regional and local scale (Storti et al., 1997; Storti and Poblet, 1997; Bigi et al., 2010 and references therein). The central zone of the basin, corresponding to

**Table 2**

Slip rate and uplift rate calculated for the Costiera anticline based on the progressive restoration resumed in Figure 9. (1) Numerical age indicates the age of the bottom of the sequences recognized in this work; the chronostratigraphic scale is the same as in Figure 5. (2) This lower interval is calculated only for the *G. puncticulata* zone that is the age of the  $S_0$  deposits involved in deformation.

Sequence	Shortening (m)	My (1)	Uplift (m)	Slip rate (mm/y)	Uplift rate (mm/y)
$S_5$		1.8	5		0.0027
$S_4$	787	2.1	174	2.62	0.58
$S_3$	520.42	3.2	142	0.47	0.129
$S_2$	684	3.6	56	1.71	0.14
$S_1$	30	3.8	180	0.15	0.9
$S_0$ (2)	641	4.6	46	0.8	0.05

the area of overlap of these two systems, is located in correspondence of a transition zone from a paleogeographic and by a structural point of view. To the north the carbonate substratum consists of the highly stratified, meso–cenozoic pelagic succession (Carminati and Santantonio, 2005) characterized by several detachment levels corresponding to marls and clay levels; to the south, it passes to a slope-to-basin succession and than to carbonate platform successions, cropping out in the surrounding Gran Sasso and the Maiella structural unit (Fig. 1). The orientation of this paleogeographic margin is oriented WNW–ESE, parallel to the main paleogeographic lineaments recognized in the central Apennines (Rusciadelli and Ricci, 2008). The structural units involving the carbonate platform succession are more uplifted, even that this structural elevation is interpreted in several different ways by the Authors (Patacca et al., 2008; Masini et al., 2011). In this area of overlap, corresponding to the Vomano valley, in the central part of the basin, this paleogeographic organization can control the location of the thrust ramp, the development of the hanging wall anticline, and the distribution of the local stress field (Figs. 2 and 7).

While in the overlap zone the two thrust system have a symmetric organization and the intermediate flat can be well

define for both the two unit, in the other two section, where just one unit is well developed, the displacement is locate at the front of this structure. As is observable in Figure 8 the front of the Nereto–Bellante is composed by several splays showing a break back sequence of deformation, and, in Figures 6 and 7, the same organization is observable for the Costiera Structure. This aspect can be related to the localization of deformation along a single structure, and to a progressive unloading during propagation, that usually triggers the development of new planes in the hanging wall of the older one (McClay and Whitehouse, 2004).

## 8. Conclusion

The development of software dedicated to 3D reconstruction such as the one used in this paper, Move 2011 (Midland Valley), provided helpful tools to better understand complex geological subsurface structures and provides useful tools also for their quantitative analysis in order to define shortening values, slip and uplift rates. In addition, these techniques are a critical support for simulation of geological processes such as earthquakes distribution, volcanic eruptions, fluid migration, in order to exploit natural resources or to evaluate natural hazard.

The geological and structural setting of the Marche–Abruzzi sector of the Periadriatic basin has been reconstructed in a 3D model through the interpolation of closely and regularly spaced 2D seismic sections, constrained by wells data and surface geology (Figs. 2 and 4). In this area, the main geological structures constitute the more external part of the Apennines fold-and-thrust belt and are mostly buried under a syn- and post-orogenic, Plio–Pleistocene, siliciclastic sequence. The seismic analysis, performed in 2D allowed to recognized in this succession six seismic sequences (Figs. 5 and 6). Their reconstruction in the third dimension allowed to recognize the occurrence of a diachronic activity along the same thrust front and to define the deformation chronology of each thrust system. The 3D model allowed us to correlate the main thrust fronts and related anticlines along strike, revealing a general ramp – flat – ramp trajectory characterizing the main structural trends. This geometric organization influences the sequence of thrust-system propagation and characterizes the evolution of syntectonic basins.

The literature recognized in this area just two front and related anticlines; our analysis pointed out that the internal trend is composed by two different thrust systems, the Nereto–Bellante thrust system in the north and the Villadegna–Costiera thrust system to the south. These two have an overlap zone corresponding to the central part of the basin, in correspondence to a paleogeographic transitional zone of the Meso–Cenozoic successions. All structures show a diachronic thrusts activity along strike, younger toward the north.

The restoration of the geological cross section obtained by the time-to-depth conversion performed with Move 2011 (Midland Valley) indicate a shortening value of about 13% corresponding to 6 km on a section of 52 km of length (Fig. 8) for the deformation acted during the Pliocene time. This value is comparable to the others shortening values calculated in this area. The forward restoration of the Costiera Structure from Early Pliocene to Quaternary allows to measure the variation of strain rate and uplift rate of this fault-related anticline.

## Acknowledgments

We are indebted to Medoil S.p.A, that provided access to part of the data used in this study. Thanks to Carlo Doglioni, Eugenio Carminati and Ernesto Centamore for their insightful comments and discussions about the geology of this sector of the Periadriatic

basin. Seismic interpretation and 3D modeling were performed using Move 2010 and 2011 made available through the Midland Valley academic grant program.

## References

- Argnani, A., Frugoni, F., 1997. Foreland deformation in the Central Adriatic and its bearing on the evolution of the Northern Apennines. *Annali di Geofisica* 40 (3), 771–780.
- Artori, A., 2007. Growth rates and two-mode accretion in the outer orogenic wedge-foreland basin system of Central Apennine (Italy). *Bollettino Società Geologica Italiana* 126, 531–556.
- Artori, A., Casero, P., 1997. Sequential balancing of growth structures, the late tertiary example from the Central Apennines. *Bulletin Societe Géologique de France* 168 (1), 35–49.
- Bally, A.W., Burbi, L., Cooper, C., Ghelardoni, R., 1986. Balanced sections and seismic reflection profiles across the central Apennines. *Memorie della Società Geologica Italiana* 35, 257–310.
- Bigi, S., Cantalamessa, G., Centamore, E., Didaskalou, P., Micarelli, A., Nisio, S., Pennesi, T., Potetti, M., 1997. The periadriatic basin (Marche–Abruzzi sector, central Italy) during the Plio–Pleistocene. *Giornale di Geologia* 59 (1–2), 245–259.
- Bigi, S., Costa Pisani, P., Argnani, A., Paltrinieri, W., 2004. Structural styles in Central Apennines: control of continental margin structures and stratigraphy on the foreland fold-and-thrust-belt architecture. Poster, 32nd IGC, Florence, 2004.
- Bigi, S., Milli, S., Corrado, S., Casero, P., Aldega, L., Botti, F., Moscatelli, M., Stanzione, O., Falcini, F., Marini, M., Cannata, D., 2009. Stratigraphy, structural setting and burial history of the Messinian Laga basin in the context of Apennine foreland basin system. *Journal of Mediterranean Earth Sciences* 1, 61–64. <http://dx.doi.org/10.3304/JMES.2009.006>.
- Bigi, S., Di Paolo, L., Vadacca, L., Gambardella, G., 2010. Load and unload as interference factors on cyclical behavior and kinematics of Coulomb wedges: insights from sandbox experiments. *Journal of Structural Geology* 32 (1), 28–44.
- Bigi, S., Casero, P., Ciotoli, G., 2011. Seismic interpretation of the Laga basin; constraints on the structural setting and kinematics of the Central Apennines. *Journal of Geological Society of London* 168, 1179–1189. <http://dx.doi.org/10.1144/0016-76492010-084>.
- Bolis, G., Carruba, S., Casnedi, R., Perotti, C.R., Ravaglia, A., Tornaghi, M., 2003. Compressional tectonics overprinting extensional structures in the Abruzzo Periadriatic Foredeep (Central Italy) during Pliocene times. *Bollettino Società Geologica Italiana* 122, 251–266.
- Carminati, E., Santantonio, M., 2005. Control of differential compaction on the geometry of sediments onlapping paleoescarpments: insights from field geology (Central Apennines, Italy) and numerical modeling. *Geology* 33 (5), 353–356.
- Carminati, E., Wortel, M.J.R., Spakman, W., Sabadini, R., 1998. The role of slab detachment processes in the opening of the western-central Mediterranean basins: some geological and geophysical evidence. *Earth and Planetary Science Letters* 160 (3–4), 651–665.
- Carruba, S., Casnedi, R., Perotti, C.R., Tornaghi, M., Bolis, G., 2006. Tectonic and sedimentary evolution of the Lower Pliocene Periadriatic foredeep in central Italy. *International Journal of Earth Sciences (Geologische Rundschau)* 95, 665–683.
- Casero, P., 2004. Structural setting of petroleum exploration plays in Italy. In: Crescenti, U., d'Offizi, S., Merlino, S., Sacchi, L. (Eds.), *Geology of Italy. Special Publication of the Italian Geological Society for the IGC 32nd*. Florence, 2004, pp. 189–199.
- Casnedi, R., 1983. Hydrocarbon-bearing submarine fan system of Cellino Formation, central Italy. *Bulletin of American Association Petroleum Geology* 67, 359–370.
- Casnedi, R., Follador, U., Moruzzi, G., 1976. *Geologia del campo gassifero di Cellino (Abruzzo)*. Bollettino Società Geologica Italiana 95, 891–901.
- Caumon, G., Collon-Drouillet, P., Le Carlier de Veslud, C., Sausse, J., Viseur, S., 2009. Surface-based 3D modeling of geological structures. *Mathematical Geosciences* 41 (9), 927–945. <http://dx.doi.org/10.1007/s11004-009-9244-2>.
- Centamore, E., Cantalamessa, G., Micarelli, A., Potetti, M., Berti, D., Bigi, S., Morelli, C., Ridolfi, M., 1991a. Stratigrafia e analisi di facies dei depositi del miocene e del pliocene inferiore dell'avanfossa marchigiano-abruzzese e delle zone limitrofe, vol. spec. CROP 11. *Studi Geologici Camerti*. 125–131.
- Centamore, E., Cantalamessa, G., Micarelli, A., Potetti, M., Berti, D., Bigi, S., Morelli, C., Ridolfi, M., 1991b. Carta geologica dei bacini della Laga e del Cellino e delle zone limitrofe. 1:100.000. Selca, Firenze.
- Courrioux, G., Nullans, S., Guillen, A., Boissonnat, J.D., 2001. 3D volumetric modeling of Cadomian terranes (Northern Brittany, France): an automatic method using Voronoi diagrams. *Tectonophysics* 331, 181–196.
- Crescenti, U., D'amato, C., Balduzzi, A., Tonna, M., 1980. Il Plio–Pleistocene del sottosuolo abruzzese-marchigiano tra Ascoli Piceno e Pescara. *Geologica Romana* 19, 63–84.
- Crescenti, U., Milia, M.L., Rusciadelli, G., 2004. Stratigraphic and tectonic evolution of the Pliocene Abruzzi basin (Central Apennines, Italy). *Bollettino Società Geologica Italiana* 123, 163–173.
- Dattilo, P., Pasi, R., Bertozzi, G., 1999. Depositional and structural dynamics of the Pliocene Peri-Adriatic Foredeep, NE Italy. *Journal of Petroleum Geology* 22, 19–36.

- DeCelles, P.G., Giles, K.A., 1996. Foreland basin systems. *Basin Research* 8, 105–123.
- Di Francesco, L., Fabbri, S., Santantonio, M., Bigi, S., Poblet, J., 2010. Contribution of different kinematic models and a complex Jurassic stratigraphy in the construction of a forward model for the Montagna dei Fiori fault-related fold (Central Apennines, Italy). *Geological Journal* 45 (5–6), 489–505.
- Doglion, C., 1991. A proposal for the kinematic modelling of W-dipping subductions-possible applications to the Tyrrhenian-Appennines system. *Terra Nova* 3, 423–434.
- Doglion, C., Gueguen, E., Sábát, F., Fernandez, M., 1997. The Western Mediterranean extensional basins and the Alpine orogen. *Terra Nova* 9 (3), 109–112.
- Flemings, P.B., Jordan, T.E., 1989. A synthetic stratigraphic model of foreland basin development. *Journal of Geophysical Research* 94 (B4), 3853–3866.
- Fonnesu, F., 2000. 3D Seismic Images of a Low-sinuosity Slope Channel and Related Depositional Lobe (West Africa Deep-offshore). ENI-Exploration and Production Division, San Donato Milanese, Italy.
- Ford, M., 2004. Depositional wedge tops: interaction between low basal friction external orogenic wedges and flexural foreland basins. *Basin Research* 16, 361–375.
- Galera, C., Tennis, C., Moretti, I., Mallet, J.L., 2003. Construction of coherent 3D geological blocks. *Computers & Geosciences* 29 (8), 971–984.
- Gee, M.J.R., Uyub, H.S., Warren, J., Morley, C.K., Lambiase, J.J., 2007. The Brunei slide: a giant submarine landslide on the North West Borneo Margin revealed by 3D seismic data. *Marine Geology* 246 (1), 9–23.
- Grandstein, F., Ogg, J., Palmer, A.R., Smith, A.G., Geissman, J., 2004. *Cenozoic Time Scale Mesozoic and Cenozoic Sequence Stratigraphy of European Basins*. Cambridge University Press, Cambridge.
- Iaccarino, S., 1985. Mediterranean Miocene and Pliocene Planktic Foraminifera. In: Bolli, H.M., Saunders, J.B., Perch-Nielsen, K. (Eds.), *Plankton Stratigraphy*. Cambridge Univ. Press, pp. 283–314.
- Keller, E.A., Zepeda, R.L., Rockwell, T.K., Ku, T.L., Dinklage, W.S., 2012. Active tectonics at Wheeler ridge, southern San Joaquin Valley, California. *GSA Bulletin* 110 (3), 298–310.
- Ledru, P., 2001. The Cadomian crust of Brittany (France): 3D imagery from multi-source data (Géofrance 3D). *Tectonophysics* 331, 300–320.
- Malinverno, A., Ryan, W.B.F., 1986. Extension of the Tyrrhenian Sea and shortening in the Apennines as a result of arc migration driven by sinking of the lithosphere. *Tectonics* 5, 227–245. <http://dx.doi.org/10.1029/TC005i002p00227>.
- Masini, M., Bigi, S., Poblet, J., Bulnes, M., Cuia, R.D., Casabianca, D., 2011. Kinematic evolution and strain simulation, based on cross-section restoration, of the Maiella Mountain: an analogue for oil fields in the Apennines (Italy). In: Poblet, J., Lisle, R.J. (Eds.), *Kinematic Evolution and Structural Styles of Fold-and-Thrust Belts*. Geological Society, London, Special Publications, vol. 349, pp. 25–44. <http://dx.doi.org/10.1144/SP349.2>.
- McClay, K.R., Whitehouse, P.S., 2004. Analogue modeling of doubly vergent thrust wedges. In: McClay, K.R. (Ed.), *Thrust Tectonics and Hydrocarbon Systems*. Memoir of American Association of Petroleum Geologists, vol. 82, pp. 184–206.
- Medwedeff, W., 1992. In: Mitra, Fisher, J. (Eds.), *Structural Geology of Fold and Thrust Belt*. Hopkins University Press, Baltimore, pp. 3–28.
- Milli, S., Moscatelli, M., 2000. Facies analysis and physical stratigraphy of the Messinian turbiditic complex in the Valle del Salto and Val di Varri (Central Apennines). *Giornale di Geologia* 62, 57–77.
- Ogg, J.G., Ogg, G., Gradstein, F.M., 2008. *The Concise Geologic Time Scale*. Cambridge University Press, 150 pp.
- Ori, G., Friend, P.F., 1984. Sedimentary basins formed and carried piggyback on active thrust sheets. *Geology* 12, 475–478.
- Ori, G., Roveri, M., Vannoni, F., 1986. Plio-Pleistocene Sedimentation in the Apenninic Adriatic Foredeep (Central Adriatic Sea, Italy). In: Special Publication, International Association Sedimentologists, vol. 8, pp. 183–198.
- Ori, G., Serafini, G., Visentin, C., Ricci Lucchi, F., Casnedi, R., Colalongo, M.L., Mosna, S., 1991. The Pliocene-Pleistocene Adriatic foredeep (Marche and Abruzzo, 110 Italy): an integrated approach to surface and subsurface geology. 3rd E.A.P.G. Conference, Adriatic Foredeep Field Trip, Guide Book (Florence, May 26th–30th, 1991), 85 pp.
- Paltrinieri, W., Zanchini, G., Martini, N., Rocca, L., 1982. Evoluzione del bacino torbiditico marchigiano-abruzzese a partire dal Messiniano in base a lineeazioni profonde. *Memorie della Società Geologica Italiana* 24, 233–242.
- Patacca, E., Scandone, P., Di Luzio, E., Cavinato, G.P., Parotto, M., 2008. Structural architecture of the Central Apennines. Interpretation of the CROP 11 seismic profile from the Adriatic coast to the orographic divide. *Tectonics* 27, TC3006. <http://dx.doi.org/10.1029/20055TC001917>.
- Pironon, B., Champanhet, J.M., 1992. Evaluation of Pliocene bright spots of the Adriatic Sea, Italy-volcanic ash or gas. *First Break* 10, 7.
- Poblet, J., Lisle, R.J., 2011. Kinematic evolution and structural styles of fold-and-thrust belts. *Geological Society Special Publication* 349, 1–24.
- Ricci Lucchi, F., 1986. The Oligocene to recent foreland basins of northern Apennines. In: Allen, P.A., Homewood, P. (Eds.), *Foreland Basins*, International Association Sedimentologists, Special Publication, vol. 8, pp. 105–139.
- Royden, L., 1988. Flexural behavior of the continental lithosphere in Italy: constraints imposed by gravity and deflection data. *Journal of Geophysical Research* 93, 7747–7766.
- Rusciadelli, G., Ricci, C., 2008. New geological constraints for the extension of the northern Apulia platform margin west of the Maiella Mt. (Central Apennines, Italy). *Bollettino della Società Geologica Italiana* 127 (2), 375–387.
- Salvi, F., Spalla, M.I., Zucali, M., Gosso, G., 2010. Three-dimensional evaluation of fabric evolution and metamorphic reaction progress in polycyclic and poly-metamorphic terrains: a case from the Central Italian Alps. *Geological Society Special Publication* 332, 173–187.
- Scisciani, V., Montefalcone, R., 2006. Coexistence of thin- and thick-skinned tectonics: an example from the Central Apennines, Italy. *Geological Society of America Special Paper* 114 (3), 33–53.
- Storti, F., Poblet, J., 1997. Growth stratal architectures associated to decollement folds and fault-propagation folds. Inferences on fold kinematics. *Tectonophysics* 282 (1–4), 353–373.
- Storti, F., Salvini, F., McClay, K., 1997. Fault-related folding in sandbox analogue models of thrust wedges. *Journal of Structural Geology* 19 (3–4 SPEC. ISS.), 583–602.
- Suppe, J., Chou, G.T., Hook, S.C., 1992. Rates of folding and faulting determined from growth strata. In: Mc Clay, K. (Ed.), *Thrust Tectonics*. Chapman and Hall, New York, pp. 105–122.
- Tozer, R.S.J., Butler, R.W.H., Chiappini, M., Corrado, S., Mazzoli, S., Speranza, F., 2006. Testing thrust tectonic models at mountain fronts: where has the displacement gone? *Journal of Geological Society of London* 163, 1–14.
- Vezzani, L., Festa, A., Ghisetti, F., 2010. Geological-Structural Map of the Central-Southern Apennines. 2 Sheets, Scale 1: 250,000. Available in digital format with the GSA Special Paper 469.
- Videpi Project, 2009. Ministry for Economic Development UNMIG – Italian Geological Society – Assomineraria. <http://unmig.sviluppoeconomico.gov.it/videpi/en/default.htm>.
- Wu, Q., Xu, H., Zou, X., 2005. An effective method for 3D geological modeling with multi-source data integration. *Computers & Geosciences* 31 (1), 35–43.
- Zampetti, A.V., Schlager, A.W., van Konijnenburg, J.H., Everts, A.J., 2004. Architecture and growth history of a Miocene carbonate platform from 3D seismic reflection data; Luconia province, offshore Sarawak, Malaysia. *Marine and Petroleum Geology* 21 (5), 517–534.
- Zanchi, A., Francesca, S., Stefano, Z., Simone, S., Graziano, G., 2009. 3D reconstruction of complex geological bodies: examples from the Alps. *Computers & Geosciences* 35 (1), 49–69. <http://dx.doi.org/10.1016/j.cageo.2007.09.003>.
- Zoetemeijer, R., Sassi, W., Roure, F., Cloetingh, S., 1992. Geology Stratigraphic and kinematic modeling of thrust evolution, northern Apennines, Italy. *Geology* 20, 1035–1038. doi:10.1130/0091-7613(1992)020<1035:SAKMOT>2.3.CO;2.